Life Sciences 325 (2023) 121753

Contents lists available at ScienceDirect

Life Sciences

journal homepage: www.elsevier.com/locate/lifescie

Medroxyprogesterone acetate-resistant endometrial cancer cells are susceptible to ferroptosis inducers

Hikaru Murakami, Masami Hayashi *, Shinichi Terada, Masahide Ohmichi

Department of Obstetrics and Gynecology, Osaka Medical and Pharmaceutical University, Osaka, Japan

ARTICLE INFO

Keywords:
Endometrial cancer
Ferroptosis
Medroxyprogesterone acetate (MPA)
SLC7A11
GPX4
Fertility-preserving treatment

ABSTRACT

Aims: Medroxyprogesterone acetate (MPA) is the most common fertility-sparing treatment in patients with early-stage endometrial cancer. If MPA treatment fails, hysterectomy is recommended. Thus, there is an urgent need for novel treatment approaches for MPA-resistant endometrial cancer patients who wish to preserve their fertility. Ferroptosis is a recently discovered type of regulated cell death caused by the excessive accumulation of reactive oxygen species (ROS), followed by aberrant lipid peroxidation. Recent studies have shown that inducing ferroptosis is a potential therapeutic strategy for cancer. However, the role of ferroptosis in endometrial cancer treatment remains to be discussed. We therefore investigated the effects of ferroptosis inducers on MPA-resistant endometrial cancer cells.

Main methods: The levels of solute carrier family 7 member 11 (SLC7A11) and glutathione peroxidase 4 (GPX4), the main mediators of ferroptosis, were examined. Cell viability was evaluated after treatment with the ferroptosis inducers sulfasalazine, erastin, or RSL3. The degree of intracellular oxidative stress after treatment with these drugs was evaluated by the glutathione level, ROS level, ferrous iron level, lipid peroxidation and changes in mitochondrial morphology. The effect of ferroptosis inducers *in vivo* was also examined.

Key findings: The expression of SLC7A11 and GPX4 in MPA-resistant ECC-1 cells decreased in comparison to parental ECC-1 cells. Sulfasalazine, erastin, and RSL3 significantly reduced cell viability and increased intracellular oxidative stress in MPA-resistant ECC-1 cells. Ferroptosis inducers also suppressed *in vivo* tumor growth more effectively in MPA-resistant ECC-1.

Significance: Treatment with ferroptosis inducers could be a novel therapeutic approach for MPA-resistant endometrial cancer.

1. Introduction

Endometrial cancer (EC) is the most common gynecological malignancy in developed countries, with >417,000 new cases and 97,000 deaths diagnosed worldwide in 2020 [24]. A large proportion of these women are diagnosed with atypical endometrial hyperplasia (AEH), a precancerous condition that can lead to overt cancer. Although EC is mostly a postmenopausal cancer, 14 %–25 % of patients are premenopausal, and 5 % are women of reproductive age [20].

Hysterectomy represents the standard management in EC and AEH. However, this treatment leads to the loss of a woman's reproductive function. Therefore, a conservative approach can be employed for patients who wish to maintain their fertility [7]. Medroxyprogesterone acetate (MPA) is the typical first-line therapy for fertility-preserving treatment of early-stage EC and AEH. The complete response rate of MPA is 82 %–89 % for early-stage EC patients and 93 %–98 % for AEH patients. However, while this approach is associated with an overall good response rate, recurrence has been reported in 25 % to 88 % of cases [21,25,33]. Hysterectomy is strongly recommended in cases of progression or the continued presence of the disease after MPA treatment [20,30]. Therefore, there is an urgent need to develop methods to target cells that do not respond to initial MPA treatment and continue to survive.

Ferroptosis is an iron-dependent regulated form of cell death. It is distinct from other forms of cell death, such as apoptosis, necrosis, and autophagy, in terms of morphology, biochemistry, and genetics. Ferroptosis is triggered by the excessive accumulation of lipid peroxidation that ultimately leads to membrane damage [12]. Recently, emerging

* Corresponding author at: Department of Obstetrics and Gynecology, Osaka Medical and Pharmaceutical University, 2-7, Daigakumachi, Takatsuki, Osaka 569-8686, Japan.
E-mail address: masami.hayashi@ompu.ac.jp (M. Hayashi).

https://doi.org/10.1016/j.lfs.2023.121753
Received 3 February 2023; Received in revised form 27 April 2023; Accepted 1 May 2023
Available online 7 May 2023

studies have reported that ferroptosis is related to the pathophysiologic processes of various diseases, such as ischemia/reperfusion injury and neurodegenerative disease [8,13]. Ferroptosis also plays an important role in cancer cells. Several studies have shown that ferroptosis typically occurs infrequently in cancer cells; however, it occurs quite frequently after chemotherapy [4,14]. In addition, an increasing number of studies have shown great interest in applying ferroptosis to cancer treatment, including colorectal cancer [28], liver cancer [16] and gastric cancer [3]. However, the utility of ferroptosis for treating EC or AEH has not yet been elucidated.

Solute carrier family 7 member 11 (SLC7A11) serves as a cystine/glutamate antiporter that transports extracellular cystine into cells. The uptake of cystine leads to conversion to cysteine, which is a rate-limiting precursor for glutathione (GSH) synthesis. GSH serves as a cofactor of glutathione peroxidase 4 (GPX4) for reducing lipid peroxidation. Thus, suppressing SLC7A11 or GPX4 has been confirmed to lead to the accumulation of lipid peroxidation, ultimately inducing ferroptosis [11].

Recent studies on several cancers have reported that drug-resistant cancer cells are more vulnerable to ferroptosis inducers than parental cells unexposed to anticancer drugs [10,29]. However, the effect of ferroptosis inducers on MPA-resistant endometrial cancer remains unknown.

The present study investigated the effect of ferroptosis inducers on MPA-resistant endometrial cancer cells both *in vitro* and *in vivo*.

2. Materials and methods

2.1. Cell and cell culture

ECC-1 cells, a well-differentiated human endometrial cancer cell line, were obtained from the American Type Culture Collection (ATCC, Manassas, VA, USA). This cell line is responsive to sex hormones with luminal characteristics that maintain estrogen receptors, progesterone receptors and androgen receptors and is commonly used as a representative type I endometrial cancer cell line [1,18]. The cells were grown in DMEM (Biological Industries, Kibbutz Beit-Haemek, Israel) supplemented with 10 % fetal bovine serum (FBS; Gibco, Thermo Fisher Scientific, Waltham, MA, USA) in an atmosphere of 5 % CO_2 and 95 % air at 37 °C.

2.2. Resistant cell derivation

Drug-resistant ECC-1 cells were prepared as described in a previous publication [6]. In brief, ECC-1 endometrial cancer cells were treated with 15 μM MPA (Fujifilm Wako Pure Chemical Corporation, Osaka, Japan) dissolved in dimethyl sulfoxide (DMSO; Fujifilm Wako Pure Chemical Corporation) in culture media for at least 14 days with fresh drug added every 3 days, which allowed a small population of quiescent cells to survive. Subsequently, the removal of MPA allowed the surviving cells to regrow. The regrown cells were then treated with 15 μM MPA again, with fresh drug added every 3 days to derive MPA-resistant cells (ECC/MPA-R).

2.3. Real-time polymerase chain reaction (RT-PCR)

Total RNA was extracted from cells using the RNeasy Mini kit (Qiagen Germantown, MD, USA), according to the manufacturer's protocol. Transcriptase (Thermo Fisher Scientific) was used to synthesize cDNA using random primers. Quantitative RT-PCR (qRT-PCR) was carried out in triplicate using the StepOne Real-Time PCR System (Applied Biosystems, Carlsbad, CA, USA). SLC7A11 (Hs00921938; Applied Biosystems) and GPX4 (Hs00157812; Applied Biosystems) were used as primers for qPCR. GAPDH (Hs02786624; Applied Biosystems) was used as an internal control in the reactions.

2.4. Western blot analyses

Total protein was lysed by Pierce RIPA Buffer (Thermo Fisher Scientific). The protein concentrations were determined using a Pierce BCA Protein Assay Kit (Thermo Fisher Scientific). Equal amounts of cell proteins were separated by sodium dodecyl sulfate-polyacrylamide gel electrophoresis and transferred to PVDF membranes. The membranes were blocked with 10 % bovine serum albumin (New England BioLabs, Ipswich, MA, USA) for 1 h at room temperature, and incubated with primary antibodies against β-actin (1:1000 dilution; Cell Signaling, Boston, MA, USA), SLC7A11 (1:200 dilution; Cell Signaling) and GPX4 (1:1000 dilution; Cell Signaling) overnight at 4 °C. After washing, the membranes were incubated with horseradish peroxidase conjugated anti-rabbit IgG (1:2000 dilution; Cell Signaling). Finally, the bands were visualized using enhanced chemiluminescence (ECL Plus; GE Healthcare Life Sciences, Pittsburgh, PA, USA). The density of the bands was quantified using ImageJ [22].

2.5. An in vitro cell viability assay

Cells were seeded in 96-well plates (4000-cells/well), cultured overnight and incubated with various concentrations of sulfasalazine (SSZ; Cayman Chemical, Ann Arbor, MI, USA, 0–800 μM), erastin (Cayman Chemical, 0–20 μM) or RSL3 (Cayman Chemical, 0–0.2 μM). Matched volumes of DMSO were used as a vehicle control. At 48 h posttreatment, the viability of cells was assessed with the CellTiter 96 AQueous (MTS) One Solution Cell Proliferation Assay (Promega, Tokyo, Japan) according to the manufacturer's protocol. After incubation with the reagent for 1 h, absorbance was recorded at 490 nm using a Varioskan Lux multimode microplate reader (Thermo Fisher Scientific).

2.6. Measurement of the reduced glutathione/glutathione disulfide (GSH/GSSG) ratio

To measure the GSH/GSSG ratio, GSH/GSSG-Glo Assay kits (Promega) were used, and the experiments were performed according to the manufacturer's instructions. In brief, cells were seeded in 96-well plates (10,000 cells/well) and cultured overnight. The cells were then incubated with SSZ (200 μM) or erastin (7.5 μM) for 24 h. Matched volumes of DMSO were used as a vehicle control. Luminescence was measured with a Varioskan Lux multimode microplate reader (Thermo Fisher Scientific).

2.7. Intracellular reactive oxygen species (ROS) measurements

Cellular ROS measurement was performed with an ROS Assay kit (DOJINDO Laboratories, Kumamoto, Japan) according to the manufacturer's protocol. In brief, cells plated in quadruplicate 96-well plates (4000-cells/well) were treated with SSZ (200 μM), erastin (7.5 μM), or matched volumes of DMSO for 1 h. Subsequently, the cells were incubated with working solution (2′,7′-dichlorodihydrofluorescein diacetate; DCFH-DA Dye working solution; DOJINDO) for 30 min. The cells were then washed with Hank's balanced salt solution (HBSS), and green fluorescence was analyzed with a Varioskan Lux microplate reader (Thermo Fisher Scientific). Furthermore, to visualize these data, the cells were observed under a fluorescence microscope (BZ-8000; Keyence, Osaka, Japan).

2.8. Measurement of the increased lipid hydroperoxides

Cellular lipid hydroperoxides were detected using the Liperfluo fluorescent probe (DOJINDO) according to the manufacturer's protocol. In brief, cells plated in 6-well plates (200000-cells/well) were treated with SSZ (200 μM), erastin (7.5 μM), RSL3 (0.05 μM), or matched volumes of DMSO for 24 h. Subsequently, the cells were washed with HBSS. Then, the cells were incubated with 3 μM Liperfluo working solution

(DOJINDO) for 30 min. After incubation, the cells were washed with HBSS and observed under a fluorescence microscope (BZ-8000). The fluorescence intensity per cell was measured using the ImageJ software program.

2.9. Intracellular Fe^{2+} measurements

Cellular Fe^{2+} measurement was performed with FerroOrange (DOJINDO) according to the manufacturer's protocol. In brief, cells plated in quadruplicate 96-well plates (10000-cells/well) were treated with SSZ (200 μM), erastin (7.5 μM), RSL3 (0.05 μM), or matched volumes of DMSO for 24 h. Subsequently, the cells were washed with HBSS. Then, the cells were incubated with 1 μM FerroOrange working solution (DOJINDO) for 30 min. After incubation, red fluorescence was analyzed with a Varioskan Lux microplate reader (Thermo Fisher Scientific). To visualize these data, the cells were observed under a fluorescence microscope (BZ-8000).

2.10. Transmission electron microscopy

The samples were fixed in phosphate-buffered 2 % glutaraldehyde, followed by 2 h in a 2 % osmium tetra-oxide ice bath. The specimens were dehydrated in graded ethanol washes (Fujifilm Wako Pure Chemical Corporation), embedded in epoxy resin (TAAB Laboratories, Berkshire, UK), and cut into ultrathin sections. These sections were then stained with uranyl acetate for 15 min and lead stain solution for 5 min (Sigma-Aldrich, Gillingham, UK), after which they were observed with a transmission electron microscope (HITACHI H-7600; Hitachi, Tokyo, Japan).

2.11. Animal experiment

Female five-week-old athymic nude mice (BALB/c nu/nu) were purchased from Japan SLC, Inc. (Hamamatsu, Japan). All of the animal studies were carried out in compliance with the guidelines of the Osaka Medical and Pharmaceutical University animal care and use committee and followed the institutional guidelines for animal welfare and experimental conduct.

ECC-1 cells and MPA-resistant ECC-1 (ECC/MPA-R) cells were injected subcutaneously into the right and left shoulders of nude mice (4×10^6-cells per mouse), respectively. The *in vivo* growth of ECC-1 (left shoulder) and ECC/MPA-R (right shoulder) xenografts was monitored by measuring their volumes with calipers and calculated using the modified ellipse formula (volume = length × $[width]^2$/ 2). When the xenograft volumes reached approximately 100 mm^3, the mice were administered SSZ (500 mg/kg) on days 9 and 21, or erastin (30 mg/kg) on days 7 and 14 in the abdominal cavity. Four mice were used for the SSZ treatment experiment, while five mice were used for the erastin treatment experiment. The mice were sacrificed at the end of the experiment, the tumors were excised, weighed, measured and fixed in formalin, and then paraffin sections were made to carry out the immunohistochemistry analyses.

2.12. Immunostaining

The paraffin-embedded xenograft tissues prepared in the previous section were subjected to immunostaining for Ki-67, SLC7A11 (1:400 dilution; Proteintech, Inc. Rosemont, USA) and GPX4 (1: 6400 dilution; Abcam plc, Cambridge, UK), as described previously [19]. The Ki-67 values were expressed as the percentage of positive cells in four randomly selected fields under a microscope (Eclipse Ci-L; Nikon, Tokyo, Japan), and the dying rates were quantified using a software program (WinROOF2021).

2.13. Statistical analyses

Each *in vitro* experiment was performed at least three times independently. The results are presented as the means ± standard errors of the means. Comparisons between two groups were carried out using Student's *t*-test with statistical significance assigned at $P < 0.05$. For *in vivo* experiments, the results are also presented as the means ± standard errors of the means, and statistical significance was assigned at $P < 0.05$ by Student's *t*-test.

3. Results

3.1. Generation of MPA-resistant ECC-1 cells

Parental ECC-1 cells (ECCs) and MPA-resistant ECC-1 cells (ECC/MPA-Rs) were subjected to 0–60 μM MPA for 48 h, and viability was measured by MTS assay, showing that ECC/MPA-Rs are resistant to MPA (Fig. 1).

3.2. The levels of SLC7A11 and GPX4 are decreased in MPA-resistant ECC-1 cells

We first examined the expression of SLC7A11 and GPX4 in parental ECC-1 cells (ECCs) and MPA-resistant ECC-1 cells (ECC/MPA-Rs). RT-qPCR and Western blotting showed that the levels of SLC7A11 and GPX4 were significantly decreased in ECC/MPA-Rs at both the mRNA and protein levels (Fig. 2A and B). The downregulation of the SLC7A11/GPX4 axis, an important antioxidant system, in MPA-resistant cells prompted us to investigate vulnerabilities in oxidative stress-induced ferroptotic cell death.

3.3. MPA-resistant ECC-1 cells are vulnerable to the ferroptosis inducers SSZ, erastin and RSL3

To investigate the effect of ferroptosis inducers on ECCs and ECC/MPA-Rs, a cell viability assay was performed. To investigate the involvement of ferroptosis, we used three drugs with different mechanisms of action in the ferroptosis induction pathway. As shown in Fig. 3A and B, treatment with SSZ or erastin, inhibitors of SLC7A11, significantly inhibited cell viability in ECC/MPA-Rs in comparison to ECCs. The GPX4 inhibitor RSL3 also inhibited cell viability in ECC/MPA-Rs in

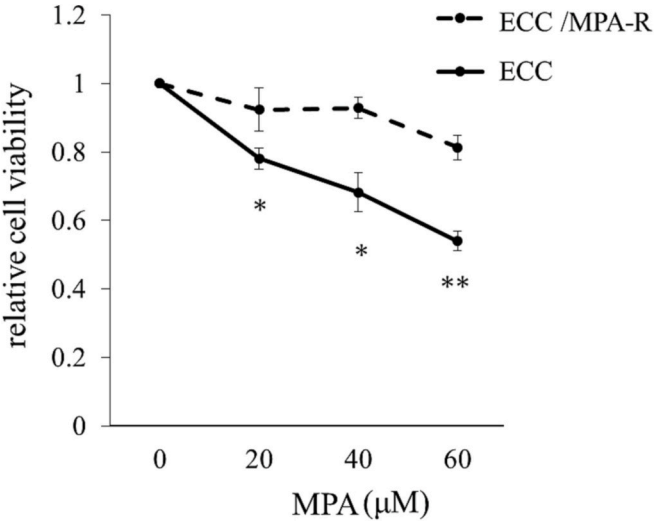

Fig. 1. Verification of MPA resistance in MPA-resistant ECC-1 cells.
Parental ECC-1 (ECC) and MPA-resistant ECC-1 (ECC/MPA-R) cells were treated with increasing concentrations of MPA for 48 h followed by MTS assay to determine cell viability. *$P < 0.05$, **$P < 0.01$.

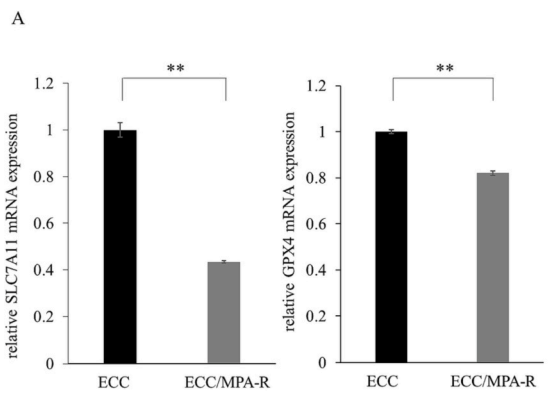

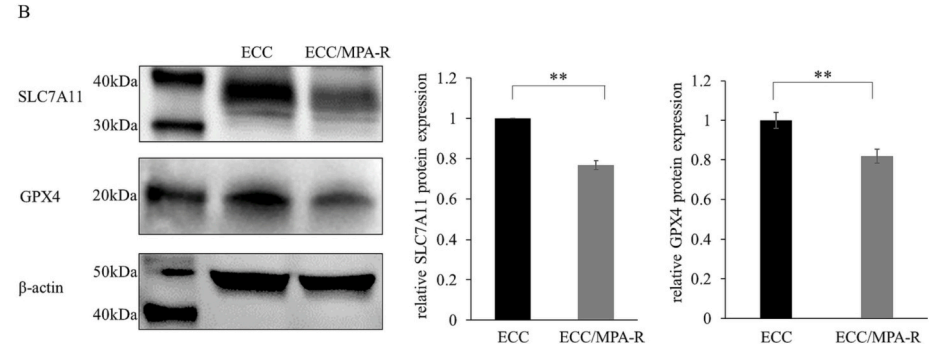

Fig. 2. SLC7A11 and GPX4 expression is down-regulated in MPA-resistant ECC-1 cells.
(A) The relative abundance of SLC7A11 and GPX4 with respect to GAPDH was calculated by qRT-PCR. (B) SLC7A11, GPX4 and β-actin (loading control) protein levels were detected by a Western blot analysis. A bar graph showing the ratio of SLC7A11 to β-actin and GPX4 to β-actin in each group. For (A) and (B), similar results were obtained in at least three independent experiments. $^{**}P < 0.01$.

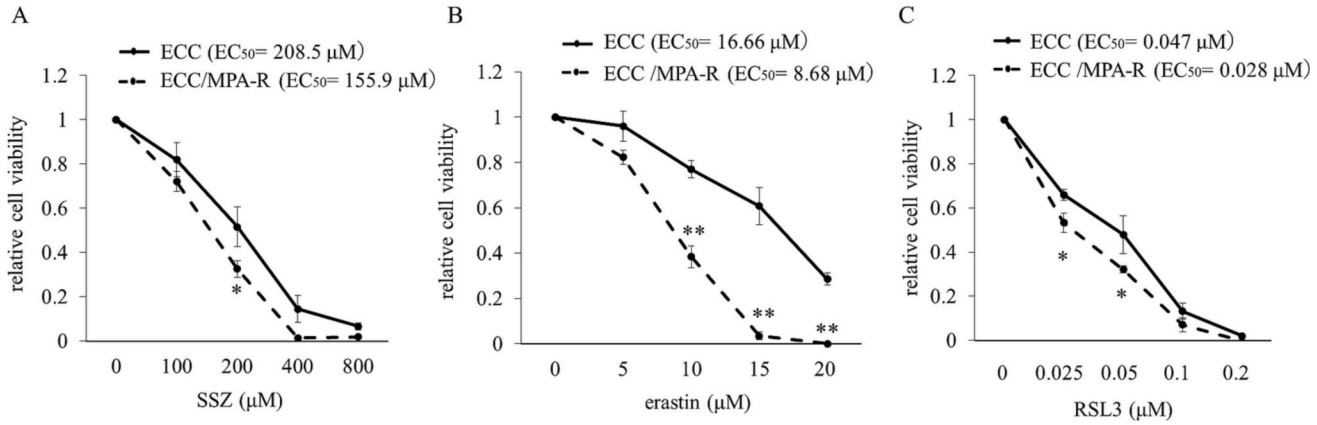

Fig. 3. MPA-resistant ECC-1 cell viability significantly decreases after the administration of ferroptosis inducers.
ECC and ECC/MPA-R cells were exposed to different doses of SSZ (A), erastin (B) or RSL3 (C) for 48 h, and cell viability was measured by an MTS assay. $^{*}P < 0.05$, $^{**}P < 0.01$.

comparison to ECCs (Fig. 3C). These results indicated that MPA-resistant ECC-1 cells have increased susceptibility to ferroptosis-inducing agents through the downregulation of the SLC7A11/GPX4 pathway.

3.4. MPA-resistant ECC-1 cells undergo ferroptosis after SSZ, erastin and RSL3 treatment

Accumulating evidence has shown that ferroptosis is ROS-dependent cell death initiated by elevated membrane lipid peroxidation. To demonstrate that this fragile characteristic of ECC/MPA-R is caused by ferroptosis, we examined the levels of lipid ROS within the cells after SSZ, erastin or RLS3 treatment. After treatment with SSZ, erastin, or RSL3, we observed an increase in the levels of ROS, with a greater increase seen in ECC/MPA-Rs than in ECCs (Fig. 4A and B). Lipid peroxidation was determined by Liperfluo staining. After treatment with SSZ, erastin, or RSL3, Liperfluo signaling was significantly increased in ECC/MPA-Rs in comparison to ECCs, indicating that ECC/MPA-Rs are more prone to lipid peroxidation reactions with ferroptosis-inducing agents (Fig. 4C and D).

GSH is a key intracellular tripeptide composed of glutamic acid, cysteine, and glycine. An enzymatic antioxidant glutathione reductase converts GSSG into GSH through the ascorbate-glutathione cycle, resulting in protection from free radical damage in cells. A reduction in the GSH/GSSG ratio is considered indicative of oxidative stress ferroptosis. To clarify the mechanism by which SSZ, erastin, or RLS3 induces oxidative stress in ECC/MPA-Rs and ECCs, we next assessed the GSH/GSSG ratio after treatment with SSZ, erastin, or RSL3. As shown in Fig. 4E, the ratio was markedly decreased in ECC/MPA-Rs in comparison to ECCs after treatment.

Given that ferroptosis is mainly dependent on intracellular iron

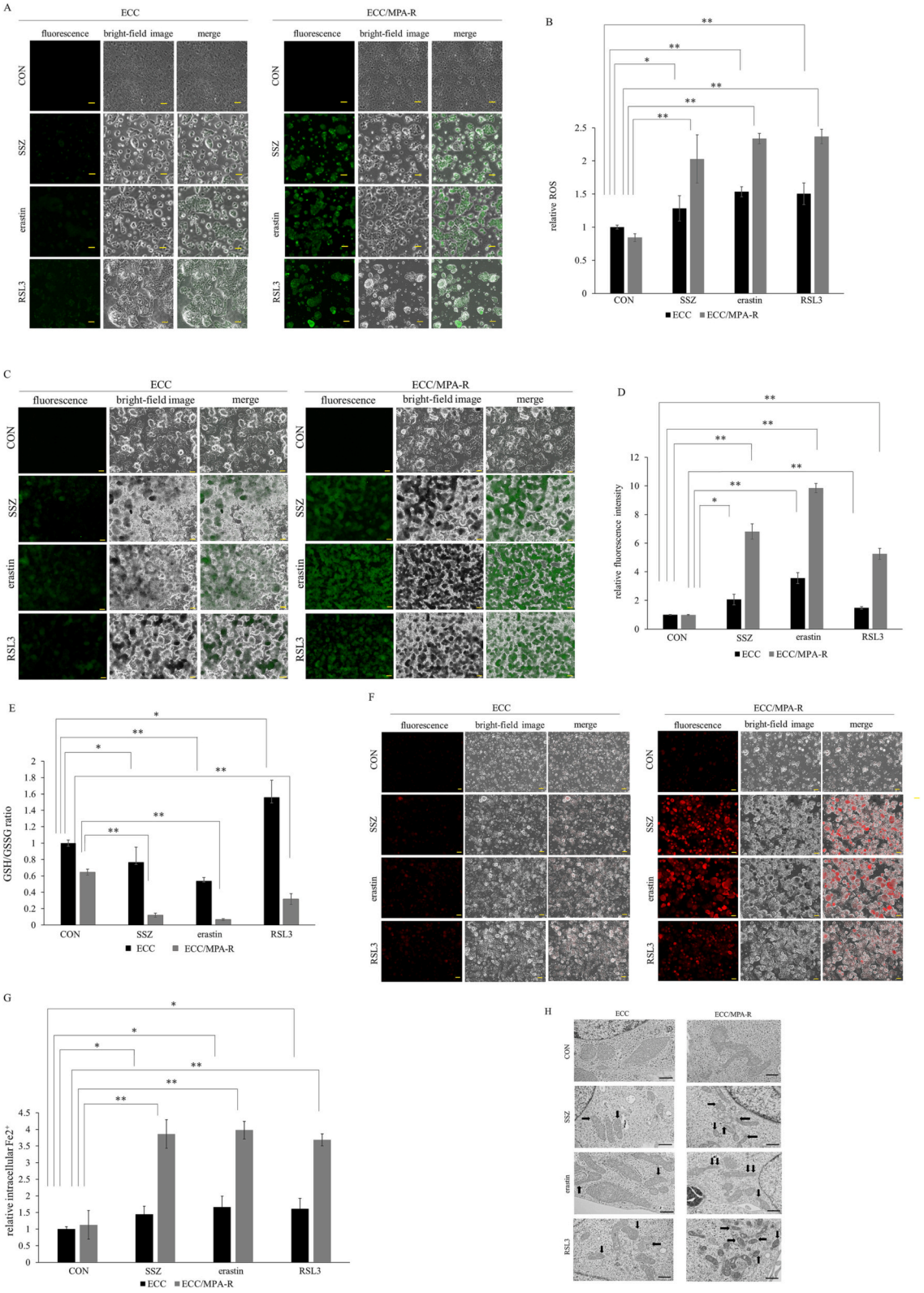

Fig. 4. SSZ-, erastin- or RSL3- induced ferroptosis significantly increases in MPA-resistant ECC-1 cells.
(A) Representative images of ROS staining in ECC and ECC/MPA-R cells. Each cell was stained with DCFH-DA probe treated without drug (CON) or with 200 μM SSZ, 7.5 μM erastin or 0.05 μM RSL3 for 1 h. Magnification x40. Scale bar: 100 μm. (B) Statistical data of the mean fluorescence intensity of DCFH-DA indicate the intracellular ROS level. The results are shown as the mean ± SD. (C) Representative images of lipid peroxidation measured by Liperfluo. (D) The fluorescence intensity was analyzed by ImageJ. The results are shown as the mean ± SD. (E) GSH/GSSH ratio. The results are shown as the mean ± SD. (F) Representative images of intracellular iron with a fluorescence microscope. (G) The intracellular divalent iron level according to the mean fluorescence intensity of FerroOrange staining. The results are shown as the mean ± SD. $*P < 0.05$, $**P < 0.01$. For (A) to (G), similar results were obtained in at least three independent experiments. (H) Transmission electron microscopy images of mitochondrial structures in ECC and ECC/MPA-R cells. Scale bar: 600 nm.

accumulation as well as lipid peroxidation, we further measured the level of intracellular divalent iron using FerroOrange probes. SSZ, erastin, or RSL3 treatment induced excessive iron content in ECC/MPA-Rs in comparison to ECCs (Fig. 4F and G).

We further performed a transmission electron microscopy assay to explore the mitochondrial morphologic changes. Treatment with SSZ, erastin, or RSL3 induced changes in mitochondrial structures, such as shrinking of the mitochondria, disappearance of the mitochondrial bilayer, and a decrease in the mitochondrial cristae, known to be ferroptotic events, and these changes were more obvious in ECC/MPA-Rs than in ECCs (Fig. 4H). These results indicate that ferroptosis by SSZ, erastin, or RLS3 is increased in ECC/MPA-Rs in comparison to ECCs through the disruption of glutathione-dependent GPX4-mediated protection from lipid peroxidation and elevated ROS.

3.5. SSZ and erastin suppress in vivo tumor growth specifically in MPA-resistant ECC-1 cells

To further verify the outcomes in *in vitro* experiments, we subsequently performed animal experiments. ECCs and ECC/MPA-Rs were injected subcutaneously into the left and right shoulders of nude mice, respectively. Subsequently, SSZ or erastin was injected into the abdominal cavity in mice (SSZ; $n = 4$, erastin; $n = 5$), and the size of the tumors was measured. After sacrifice, the tumors were harvested and weighed. The administration of SSZ led to significant differences in the tumor volume and tumor weight between ECC and ECC/MPA-R tumors (Figs. 5A to D).

To further assess the proliferation of ECC and ECC/MPA-R tumors, the tumors were fixed in formalin, and paraffin sections were examined by immunohistochemistry using an antibody against Ki-67, a marker of proliferating cells. As shown in Fig. 5E, the relative rate of Ki67-positive cells was markedly decreased in ECC/MPA-R tumors in comparison to parental ECC tumors after administration of SSZ in mice. We also examined the expression levels of ferroptosis-related genes in tumors. Immunostaining of tumor tissue revealed the decreased expression of SLC7A11 and GPX4 in tumors derived from ECC/MPA-Rs in comparison to tumors derived from ECCs (Fig. 5F). The treatment of mice with erastin showed similar results to the treatment with SSZ (Figs. 6A to F). These data indicate that ferroptosis inducers can act as tumor inhibitors with regard to the growth of MPA-resistant EC, both *in vitro* and *in vivo* and that inducing ferroptosis might be a new therapeutic approach for MPA-resistant EC.

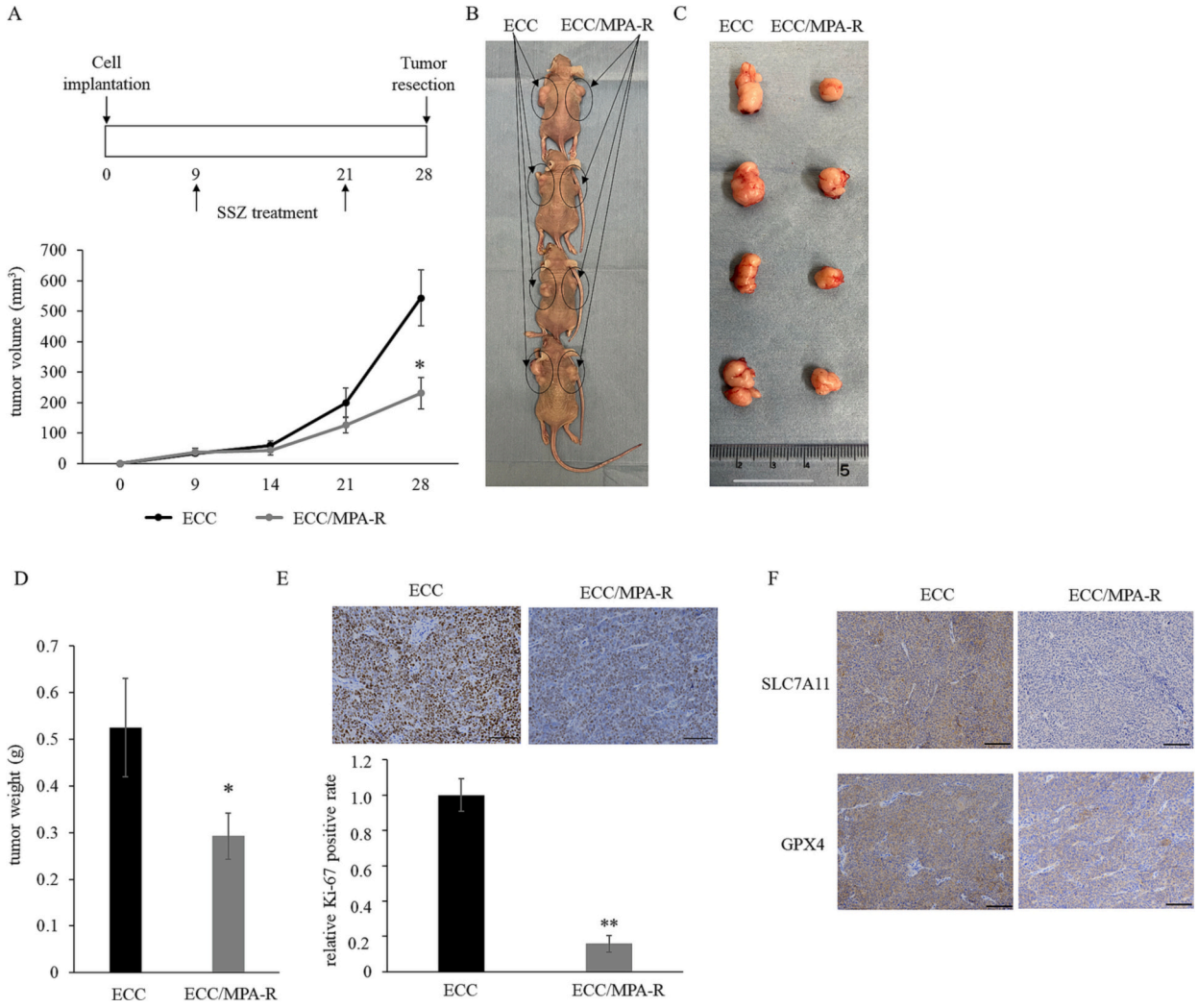

Fig. 5. Tumor growth of MPA-resistant ECC-1 cells was significantly suppressed by SSZ.
(A) The tumor volume was measured, and each value represents the mean volume ± SD. $n = 4$ (B) Images of xenograft mice 28 days after the injection of ECC-1 (left shoulder) and ECC/MPA-R (right shoulder) cells in each mouse. (C) Images of xenograft tumors. (D) Tumors were excised and weighed on day 28. (E) Immunohistochemistry of Ki-67 expression in xenograft tumors. The relative rates of Ki-67-positive cells were evaluated in the tumor tissues. (F) An immunohistochemical analysis of SLC7A11 and GPX4 expression in xenograft tumors. Magnification x 200. Scale bar: 100 μm. $^{*}P < 0.05$, $^{**}P < 0.01$.

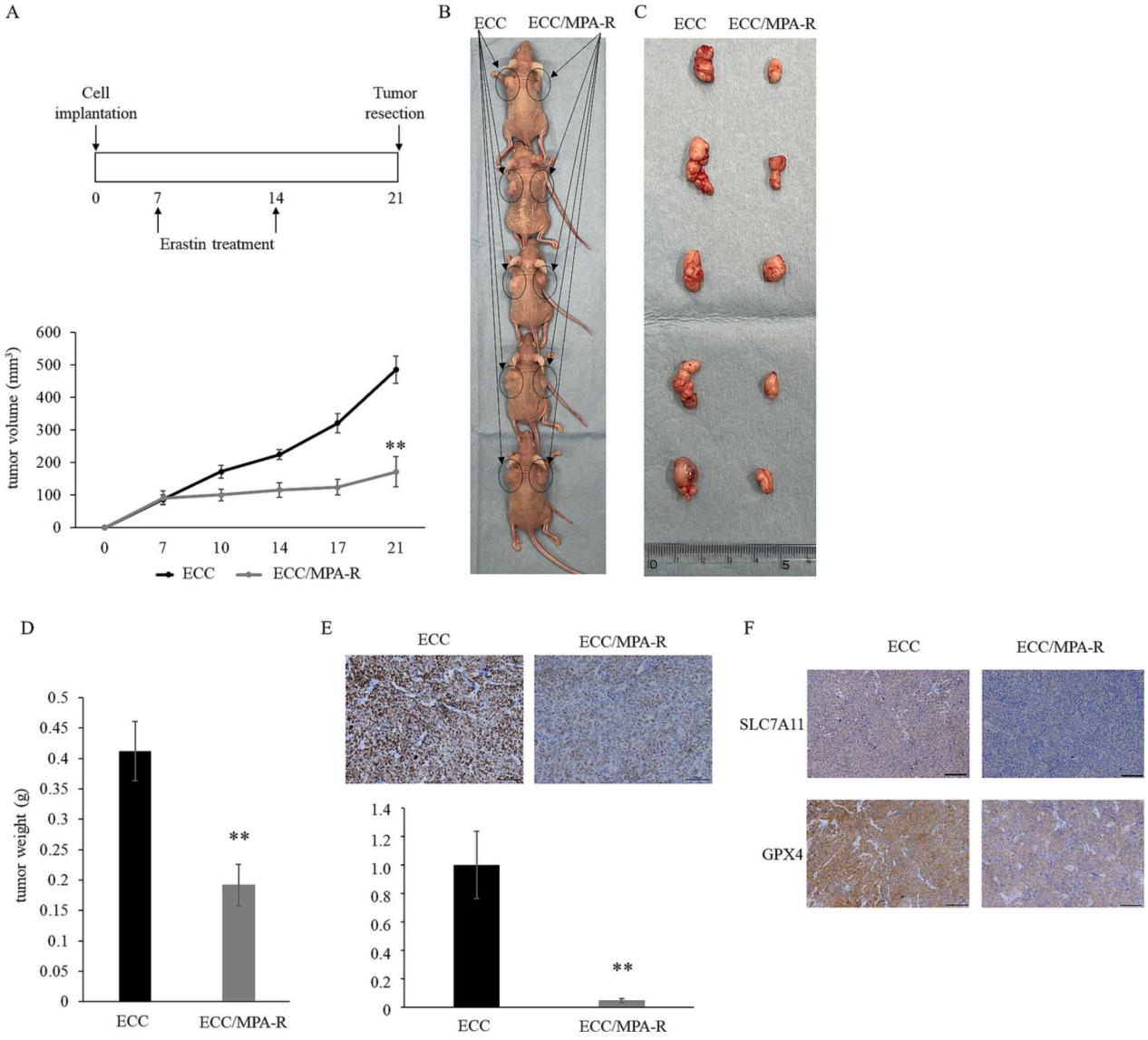

Fig. 6. Tumor growth of MPA-resistant ECC-1 cells was significantly suppressed by erastin.
(A) The tumor volume was measured and each value represents the mean volume ± SD. $n = 5$ (B) Images of xenograft mice 21 days after the injection of ECC-1 (left shoulder) and ECC/MPA-R (right shoulder) cells in each mouse. (C) Images of xenograft tumors. (D) Tumors were excised and weighed on day 21. (E) Immunohistochemistry of Ki-67 expression in xenograft tumors. The relative rates of Ki-67-positive cells were evaluated in the tumor tissues. (F) An immunohistochemical analysis of SLC7A11 and GPX4 expression in xenograft tumors. Magnification x 200. Scale bar: 100 μm. **P < 0.01.

4. Discussion

MPA administration facilitated the preservation of fertility in patients with either AEH or early-stage EC. However, MPA resistance is often an obstacle to the successful treatment of these patients because of the presence of resistant strains and a relatively high recurrence rate. Ferroptosis is a newly recognized form of regulated cell death involving cellular iron accumulation and lipid peroxidation. Increasing evidence suggests that triggering ferroptosis contributes to tumor suppression [4]. In addition, recent reports have shown that several therapy-resistant cancer cells exhibit increased sensitivity to ferroptosis inducers. Viswanathan et al. showed that gefinitib-resistant non-small cell lung cancer cells were particularly vulnerable to ferroptotic cell death induced by GPX4 inhibitors, such as RSL3 and ML210, in comparison to parental lung cancer cells [27]. Tsoi et al. reported that drug-resistant dedifferentiated melanoma cells showed increased sensitivity to the ferroptosis-inducing drugs erastin and RSL3 [26]. In paclitaxel-tolerant head and neck cancer cells, persistent cells were sensitive to SSZ and erastin but not RSL3 [34]. However, the effect of ferroptosis induction on MPA-resistant endometrial cancer still remains undetermined.

The SLC7A11/GPX4 pathway has been shown to act as a legitimate defense against ferroptosis by assisting intracellular GSH synthesis and mitigating lipid peroxidation. SLC7A11 is a multiple transmembrane protein that mediates intracellular glutamine acid export and extracellular cystine import. After cystine is absorbed into the cell, it is reduced to cysteine, the rate-limiting precursor for glutathione (GSH) synthesis. GPX4 mediates the conversion of lipid peroxides to lipid alcohols in the presence of GSH; the inhibition of SLC7A11 depletes GSH and downregulates GPX4, resulting in plasma membrane damage due to iron-dependent lipid peroxide accumulation [31]. Indeed, suppression of SLC7A11 has been shown to upregulate ferroptosis [32]. The SLC7A11/GPX4 pathway is therefore an important inhibitory pathway for ferroptosis, and has therefore attracted attention as a potential therapeutic agent. In the present study, we first demonstrated that the expression of both SLC7A11 and GPX4 significantly decreased in MPA-resistant ECC-1 EC cells in comparison to parental ECC-1 cells. We further revealed that

MPA-resistant ECC-1 cells were extremely vulnerable to ferroptosis inducers, such as SLC7A11 inhibitors and GPX4 inhibitors, in comparison to parental ECC-1 cells both *in vitro* and *in vivo*. These data suggest that ferroptosis induction *via* the suppression of the SLC7A11/GPX4 pathway may be a new approach for managing MPA-resistant EC as a fertility-preserving treatment.

In several solid tumors such as gastric cancer [17] and urothelial cancer [9], SLC7A11 is stabilized by combining with CD44 variants on the tumor cell surface, leading to increased SLC7A11 levels. In these cancers, a high expression of SLC7A11 has been demonstrated to be associated with a poor prognosis, but not in MPA-resistant EC. In other cancer types, MDA-MB-231, which is commonly used as a triple-negative breast cancer cell line model, expresses higher levels of SLC7A11. In contrast, the MCF-7 breast cancer cell line, which expresses estrogen and progesterone receptors, expresses lower levels of SLC7A11 [35]. Furthermore, Ge et al. reported that SLC7A11 is downregulated in adriamycin-resistant MCF-7 cells [6]. These differences may be due to the different expression levels of SLC7A11 in different cell types.

In the present study, we reported that SSZ, an inhibitor of SLC7A11, is effective for shrinking tumors consisting of MPA-resistant EC cells. Importantly, SSZ is commonly used to treat rheumatoid arthritis and inflammatory bowel disease in the clinical setting [15,23]. No significant association has been reported between the use of SSZ and subfertility in women (defined as time-to-conception) [2]. The present results therefore support SSZ as a novel strategy for clinical application in fertility-sparing EC therapy.

Not only early-stage EC but also AEH are indicated for MPA therapy as a fertility-preserving treatment. Because an AEH-derived cell line has not yet been established, basic research on AEH is poorly studied despite it being refractory to existing treatments. However, if we consider AEH to be a precancerous condition of EC, SSZ, erastin or RSL3 may be useful for treating MPA-resistant AEH, similar to EC. To confirm this, additional studies should be performed with clinical specimens and patient-derived xenograft models.

Several limitations associated with the present study warrant mention. The current study did not examine the mechanisms underlying how MPA-resistant ECC cells become vulnerable to ferroptosis inducers. In a previous report, the upregulation of progesterone receptor membrane component 1-related free fatty acid increase was shown to be involved in the increased sensitivity of paclitaxel-resistant head and neck cancer to ferroptosis inducers [34]. In platinum-resistant ovarian cancer cells, the improved sensitivity to ferroptosis inducers was dependent on the increase in Frizzled class receptor 7 levels [29]. To confirm how MPA-resistant EC cells became vulnerable to ferroptosis inducers, further investigations are needed.

Taken together, our findings suggest that MPA-resistant EC cells are vulnerable to the ferroptosis inducers SSZ, erastin and RSL3. Ferroptosis inducers may thus be viable novel anticancer treatments for early-stage EC.

5. Conclusion

Through the present study, we obtained new insights regarding the important role of ferroptosis inducers against MPA-resistant EC for the first time. Furthermore, ferroptosis inducers inhibit the growth of EC tumors, specifically MPA-resistant EC, implying the great potential of ferroptosis induction as a novel therapy for MPA-resistant EC patients who desire to preserve their fertility.

CRediT authorship contribution statement

Hikaru Murakami: Investigation, Formal analysis, Writing-original draft. Masami Hayashi: Conceptualization Methodology, Project administration, Writing-original draft, Writing-review & editing. Shinichi Terada: Investigation, Visualization, Writing- review & editing. Masahide Ohmichi: Validation, Supervision, Writing-review & editing. All authors read and approved the final version of the manuscript.

Funding

This research did not receive any specific grant from funding agencies in the public, commercial, or not-for-profit sectors.

Declaration of competing interest

None.

Data availability

Data will be made available on request.

References

[1] D. Aizen, M. Pasmanik-Chor, R. Sarfstein, Z. Laron, I. Bruchim, H. Werner, Genome-wide analyses identify filamin-A as a novel downstream target for insulin and IGF1 action, Front. Endocrinol. 9 (2018) 105, https://doi.org/10.3389/fendo.2018.00105. Lausanne.

[2] J. Brouwer, J.M. Hazes, J.S. Laven, R.J. Dolhain, Fertility in women with rheumatoid arthritis: influence of disease activity and medication, Ann. Rheum. Dis. 74 (2015) 1836–1841, https://doi.org/10.1136/annrheumdis-2014-205383.

[3] L. Chen, L. Qiao, Y. Bian, X. Sun, GDF15 knockdown promotes erastin-induced ferroptosis by decreasing SLC7A11 expression, Biochem. Biophys. Res. Commun. 526 (2020) 293–299, https://doi.org/10.1016/j.bbrc.2020.03.079.

[4] X. Chen, R. Kang, G. Kroemer, D. Tang, Broadening horizons: the role of ferroptosis in cancer, Nat. Rev. Clin. Oncol. 18 (2021) 280–296, https://doi.org/10.1038/s41571-020-00462-0.

[6] C. Ge, B. Cao, D. Feng, F. Zhou, J. Zhang, N. Yang, S. Feng, G. Wang, J. Aa, The downregulation of SLC7A11 enhances ROS induced P-gp overexpression and drug resistance in MCF-7 breast cancer cells, Sci. Rep. 7 (2017) 3791, https://doi.org/10.1038/s41598-017-03881-9.

[7] G. Gullo, A. Etrusco, G. Cucinella, A. Perino, V. Chiantera, A.S. Laganà, R. Tomaiuolo, A. Vitagliano, P. Giampaolino, M. Noventa, A. Andrisani, G. Buzzaccarini, Fertility-sparing approach in women affected by stage I and low-grade endometrial carcinoma: an updated overview, Int. J. Mol. Sci. 22 (2021) 11825, https://doi.org/10.3390/ijms222111825.

[8] Y. Guo, W. Zhang, X. Zhou, S. Zhao, J. Wang, Y. Guo, Y. Liao, H. Lu, J. Liu, Y. Cai, J. Wu, M. Shen, Roles of ferroptosis in cardiovascular diseases, Front. Cardiovasc. Med. 9 (2022), 911564, https://doi.org/10.3389/fcvm.2022.911564 eCollection 2022.

[9] M. Hagiwara, E. Kikuchi, N. Tanaka, T. Kosaka, S. Mikami, H. Saya, M. Oya, Variant isoforms of CD44 involves acquisition of chemoresistance to cisplatin and has potential as a novel indicator for identifying a cisplatin-resistant population in urothelial cancer, BMC Cancer 18 (2018) 113, https://doi.org/10.1186/s12885-018-3988-3.

[10] M.J. Hangauer, V.S. Viswanathan, M.J. Ryan, D. Bole, J.K. Eaton, A. Matov, J. Galeas, H.D. Dhruv, M.E. Berens, S.L. Schreiber, F. McCormick, M.T. McManus, Drug-tolerant persister cancer cells are vulnerable to GPX4 inhibition, Nature 551 (2017) 247–250, https://doi.org/10.1038/nature24297.

[11] J. He, X. Wang, K. Chen, M. Zhang, J. Wang, The amino acid transporter SLC7A11-mediated crosstalk implicated in cancer therapy and the tumor microenvironment, Biochem. Pharmacol. 205 (2022), 115241, https://doi.org/10.1016/j.bcp.2022.115241.

[12] X. Jiang, B.R. Stockwell, M. Conrad, Ferroptosis: mechanisms, biology and role in disease, Nat. Rev. Mol. Cell Biol. 22 (2021) 266–282, https://doi.org/10.1038/s41580-020-00324-8.

[13] C.J. Ko, S.L. Gao, T.K. Lin, P.Y. Chu, H.Y. Lin, Ferroptosis as a major factor and therapeutic target for neuroinflammation in Parkinson's disease, Biomedicines 9 (2021) 1679, https://doi.org/10.3390/biomedicines9111679.

[14] C. Liang, X. Zhang, M. Yang, X. Dong, Recent progress in ferroptosis inducers for cancer therapy, Adv. Mater. 31 (2019), e1904197, https://doi.org/10.1002/adma.201904197.

[15] G.R. Lichtenstein, E.V. Loftus, K.L. Isaacs, M.D. Regueiro, L.B. Gerson, B.E. Sands, ACG clinical guideline: management of Crohn's disease in adults, Am. J. Gastroenterol. 113 (2018) 481–517, https://doi.org/10.1038/ajg.2018.27.

[16] Y. Liu, L. Ouyang, C. Mao, Y. Chen, T. Li, N. Liu, Z. Wang, W. Lai, Y. Zhou, Y. Cao, S. Liu, Y. Liang, M. Wang, S. Liu, L. Chen, Y. Shi, D. Xiao, Y. Tao, PCDHB14 promotes ferroptosis and is a novel tumor suppressor in hepatocellular carcinoma, Oncogene (2022), https://doi.org/10.1038/s41388-022-02370-2 in press.

[17] S. Miyoshi, H. Tsugawa, J. Matsuzaki, K. Hirata, H. Mori, H. Saya, T. Kanai, H. Suzuki, Inhibiting xCT improves 5-fluorouracil resistance of gastric cancer induced by CD44 variant 9 expression, Anticancer Res. 38 (2018) 6163–6170, https://doi.org/10.21873/anticanres.12969.

[18] B. Mo, A.E. Vendrov, W.A. Palomino, B.R. DuPont, K.B.C. Apparao, B.A. Lessey, ECC-1 cells: a well-differentiated steroid-responsive endometrial cell line with characteristics of luminal epithelium, Biol. Reprod. 75 (2006) 387–394, https://doi.org/10.1095/biolreprod.106.051870.

[19] M. Nakamura, M. Hayashi, H. Konishi, M. Nunode, K. Ashihara, H. Sasaki, Y. Terai, M. Ohmichi, MicroRNA-22 enhances radiosensitivity in cervical cancer cell lines via direct inhibition of c-myc binding protein, and the subsequent reduction in hTERT expression, Oncol. Lett. 19 (2020) 2213–2222, https://doi.org/10.3892/ol.2020.11344.

[20] A. Obermair, E. Baxter, D.J. Brennan, J.N. McAlpine, J.J. Muellerer, F. Amant, M. D.J.M. van Gent, R.L. Coleman, S.N. Westin, M.S. Yates, C. Krakstad, M. Janda, Fertility-sparing treatment in early endometrial cancer: current state and future strategies, Obstet. Gynecol. Sci. 63 (2020) 417–431, https://doi.org/10.5468/ogs.19169.

[21] Y. Qin, Z. Yu, J. Yang, D. Cao, M. Yu, Y. Wang, K. Shen, Oral progestin treatment for early-stage endometrial cancer, Int. J. Gynecol. Cancer 26 (2016) 1081–1091, https://doi.org/10.1097/IGC.0000000000000723.

[22] C.A. Schneider, W.S. Rasband, K.W. Eliceiri, NIH image to ImageJ: 25 years of image analysis, Nat. Methods 9 (2012) 671–675, https://doi.org/10.1038/nmeth.2089.

[23] J.S. Smolen, R.B.M. Landewé, S.A. Bergstra, A. Kerschbaumer, A. Sepriano, D. Aletaha, R. Caporali, C.J. Edwards, K.L. Hyrich, J.E. Pope, S. de Souza, T. A. Stamm, T. Takeuchi, P. Verschueren, K.L. Winthrop, A. Balsa, J.M. Bathon, M. H. Buch, G.R. Burmester, F. Buttgereit, M.H. Cardiel, K. Chatzidionysiou, C. Codreanu, M. Cutolo, A.A. den Broeder, K. El Aoufy, A. Finckh, J.E. Fonseca, J. E. Gottenberg, E.A. Haavardsholm, A. Iagnocco, K. Lauper, Z. Li, I.B. McInnes, E. F. Mysler, P. Nash, G. Poor, G.G. Ristic, F. Rivellese, A. Rubbert-Roth, H. Schulze-Koops, N. Stoilov, A. Strangfeld, Mil A. van der Helm-van, E. van Duuren, T.P. M. Vliet Vlieland, R. Westhovens, D. van der Heijde, EULAR recommendations for the management of rheumatoid arthritis with synthetic and biological disease-modifying antirheumatic drugs: 2022 update, Ann. Rheum. Dis. 82 (2023) 3–18, https://doi.org/10.1136/ard-2022-223356.

[24] H. Sung, J. Ferlay, R.L. Siegel, M. Laversanne, I. Soerjomataram, A. Jemal, F. Bray, Global cancer statistics 2020: GLOBOCAN estimates of incidence and mortality worldwide for 36 cancers in 185 countries, CA Cancer J. Clin. 71 (2021) 209–249, https://doi.org/10.3322/caac.21660.

[25] S. Tamauchi, H. Kajiyama, F. Utsumi, S. Suzuki, K. Niimi, J. Sakata, M. Mizuno, K. Shibata, F. Kikkawa, Efficacy of medroxyprogesterone acetate treatment and retreatment for atypical endometrial hyperplasia and endometrial cancer, J. Obstet. Gynecol. Res. 44 (2018) 151–156, https://doi.org/10.1111/jog.13473.

[26] J. Tsoi, L. Robert, K. Paraiso, C. Galvan, K.M. Sheu, J. Lay, D.J.L. Wong, M. Atefi, R. Shirazi, X. Wang, D. Braas, C.S. Grasso, N. Palaskas, A. Ribas, T.G. Graeber, Multistage differentiation defines melanoma subtypes with differential vulnerability to drug-induced iron-dependent oxidative stress, Cancer Cell. 33 (2018) 890–904.e5, https://doi.org/10.1016/j.ccell.2018.03.017.

[27] V.S. Viswanathan, M.J. Ryan, H.D. Dhruv, S. Gill, O.M. Eichhoff, B. Seashore-Ludlow, S.D. Kaffenberger, J.K. Eaton, K. Shimada, A.J. Aguirre, S.R. Viswanathan, S.C. Chattopadhyay, P. Tamayo, W.S. Yang, M.G. Rees, S. Chen, Z.V. Boskovic, S. Javaid, C. Huang, X. Wu, Y.Y. Tseng, E.M. Roider, D. Gao, J.M. Cleary, B. M. Wolpin, J.P. Mesirov, D.A. Haber, J.A. Engelman, J.S. Boehm, J.D. Kotz, C. S. Hon, Y. Chen, W.C. Hahn, M.P. Levesque, J.G. Doench, M.E. Berens, A.F. Shamji, P.A. Clemons, B.R. Stockwell, S.L. Schreiber, Dependency of a therapy-resistant state of cancer cells on a lipid peroxidase pathway, Nature 547 (2017) 453–457, https://doi.org/10.1038/nature23007.

[28] R. Wang, Q. Su, H. Yin, D. Wu, C. Lv, Z. Yan, Inhibition of SRSF9 enhances the sensitivity of colorectal cancer to erastin-induced ferroptosis by reducing glutathione peroxidase 4 expression, Int. J. Biochem. Cell Biol. 134 (2021), 105948, https://doi.org/10.1016/j.biocel.2021.105948.

[29] Y. Wang, G. Zhao, S. Condello, H. Huang, H. Cardenas, E.J. Tanner, J. Wei, Y. Ji, J. Li, Y. Tan, R.V. Davuluri, M.E. Peter, J.X. Cheng, D. Matei, Frizzled-7 identifies platinum-tolerant ovarian cancer cells susceptible to ferroptosis, Cancer Res. 81 (2021) 384–399, https://doi.org/10.1158/0008-5472.CAN-20-1488.

[30] J. Wei, W. Zhang, L. Feng, W. Gao, Comparison of fertility-sparing treatments in patients with early endometrial cancer and atypical complex hyperplasia: a meta-analysis and systematic review, Medicine (Baltimore) 96 (2017), e8034, https://doi.org/10.1097/MD.0000000000008034.

[31] X. Wu, Y. Li, S. Zhang, X. Zhou, Ferroptosis as a novel therapeutic target for cardiovascular disease, Theranostics 11 (2021) 3052–3059, https://doi.org/10.7150/thno.54113.

[32] Y. Xie, W. Hou, X. Song, Y. Yu, J. Huang, X. Sun, R. Kang, D. Tang, Ferroptosis: process and function, Cell Death Differ. 23 (2016) 369–379, https://doi.org/10.1038/cdd.2015.158.

[33] W. Yamagami, N. Susumu, T. Makabe, K. Sakai, H. Nomura, F. Kataoka, A. Hirasawa, K. Banno, D. Aoki, Is repeated high-dose medroxyprogesterone acetate (MPA) therapy permissible for patients with early stage endometrial cancer or atypical endometrial hyperplasia who desire preserving fertility? J. Gynecol. Oncol. 29 (2018), e21 https://doi.org/10.3802/jgo.2018.29.e21.

[34] J.H. You, J. Lee, J.L. Roh, PGRMC1-dependent lipophagy promotes ferroptosis in paclitaxel-tolerant persister cancer cells, J. Exp. Clin. Cancer Res. 40 (2021) 350, https://doi.org/10.1186/s13046-021-02168-2.

[35] M.C. Chen, L.L. Hsu, S.F. Wan, C.Y. Hsu, H.C. Lee, L.M. Tseng, ROS mediate xCT-dependent cell death in human breast cancer cells under glucose deprivation, Cells 9 (2020) 1598, https://doi.org/10.3390/cells9071598.